

## Quiescence as a mechanism for cyclical hypoxia and acidosis

Kieran Smallbone · David J. Gavaghan ·  
Philip K. Maini · J. Michael Brady

Received: 14 August 2006 / Revised: 15 February 2007 / Published online: 3 July 2007  
© Springer-Verlag 2007

**Abstract** Tumour tissue characteristically experiences fluctuations in substrate supply. This unstable microenvironment drives constitutive metabolic changes within cellular populations and, ultimately, leads to a more aggressive phenotype. Previously, variations in substrate levels were assumed to occur through oscillations in the haemodynamics of nearby and distant blood vessels. In this paper we examine an alternative hypothesis, that cycles of metabolite concentrations are also driven by cycles of cellular quiescence and proliferation. Using a mathematical modelling approach, we show that the interdependence between cell cycle and the microenvironment will induce typical cycles with the period of order hours in tumour acidity and oxygenation. As a corollary, this means that the standard assumption of metabolites entering diffusive equilibrium around the tumour is not valid; instead temporal dynamics must be considered.

---

This research was partially funded by EPSRC grant GR/R96149/01 “The Oxford University Life Sciences Interface Doctoral Training Centre” and BBSRC grant BB/C008219/1 “The Manchester Centre for Integrative Systems Biology (MCISB)”. We thank the referees for their suggestions during the preparation of the final manuscript.

---

K. Smallbone (✉)

Manchester Centre for Integrative Systems Biology, Manchester Interdisciplinary Biocentre,  
131 Princess Street, Manchester, M1 7DN, UK  
e-mail: kieran.smallbone@manchester.ac.uk

D. J. Gavaghan

Oxford University Computing Laboratory, Parks Road, Oxford, OX1 3QD, UK

P. K. Maini

Centre for Mathematical Biology, Mathematical Institute, University of Oxford,  
24–29 St Giles’, Oxford, OX1 3LB, UK

J. M. Brady

Department of Engineering Science, University of Oxford, Parks Road, Oxford, OX1 3PJ, UK

**Keywords** Acidity · Hypoxia · Delay differential equations

**Mathematics Subject Classification (2000)** 92B99 · 35K57

## 1 Introduction

Many aggressive tumours show increased reliance on glycolysis to produce energy, even in the presence of sufficient oxygen [26]. Subsequent investigations have shown that this characteristic, known as aerobic glycolysis, may play a critical role in the transition from benign to malignant growth [8, 23, 24]. A key factor in the adoption of aerobic glycolysis by tumour cell populations is their exposure to an unstable microenvironment, experiencing oscillations in substrate supply. For example, normoxic–hypoxic cycles in tumours have been measured to occur with periodicities of minutes [14], hours [12] and days [9]. From a bioenergetic perspective, those cells in which aerobic glycolysis is constitutively upregulated will be better placed to respond to these periods of hypoxia, and thus positively selected by somatic evolutionary pressures.

Using a magnetic resonance imaging (MRI) technique that is sensitive to oxygen levels, oscillations in signal intensity (oxygenation) have been shown to occur with periodicities of both one and twenty cycles per hour [1]. Contrastingly, using microelectrodes, oxygenation cycles have been measured with periodicities of 1–2 per min [2]. These discrepancies may be explained because MRI is relatively insensitive to rapid fluctuations, whilst instabilities in microelectrodes mean this modality is insensitive to slower changes [8].

Each of the studies mentioned above shows that tumour cells experience considerable changes in oxygen delivery. The primary explanation put forward for transient hypoxia and reoxygenation is oscillations in the haemodynamics, or blood delivery, of nearby and distant vessels [8, 13]. Rapid normoxic–hypoxic cycles are thought to occur due to fluctuations in haematocrit, the concentration of red cells in the blood [5], or through vasomotion, rhythmic oscillations in vessel diameter [25]. Longer cycles, occurring over days, are likely to be due to vascular remodelling, the active process of altering the structure and arrangement of blood vessels [13, 19]. Vascular remodelling is driven by cycles of angiogenesis promoted by hypoxia-induced expression of vascular endothelial growth factor (VEGF), an induction and survival factor for new blood vessels [9].

In this paper, we examine an alternative mechanism for the observed substrate oscillations in tumour tissue, namely cellular quiescence. High levels of acidity can induce cells to cease proliferation, i.e. become quiescent [4]. Specifically, acidosis promotes the production of hypoxia inducible factor 1 (HIF-1); via a cyclin-dependent kinase inhibitor, p27, HIF-1 acts to inhibit the cell-cycle [10, 18]. Quiescent cells are essentially metabolically inactive, producing significantly less acid than their proliferating counterparts. Thus the level of acidity will decrease, allowing cells to resume proliferation. We demonstrate that this simple feedback mechanism may produce the observed cycles in tumour substrate levels. Whilst our focus is on growth inhibitors produced by tumour tissue, such as lactic acid, the analysis is equally valid for growth promoters consumed by tumour tissue, such as oxygen.

## 2 Model development

We model the tumour as a sphere of radius  $R_M$  and assume that spherical symmetry prevails at all times. We consider first the dynamics of acidity in and around the tumour, though later we shall show that the analysis holds for the dynamics of other substrates, such as oxygen.

Let  $H$  denote the extracellular concentration of excess hydrogen ions, where excess means above its normal level of  $10^{-7.25}\text{M} \equiv \text{pH } 7.25$ . We assume that there exists a sharp acidity threshold  $H_Q$  above which tumour cells cease proliferation. Define the acid production rate  $r_H = \phi_Q$  per unit volume for quiescent cells and  $r_H = \phi_A$  for active cells, where  $\phi_Q \ll \phi_A$  as quiescent cells are relatively inactive. The vascular density is taken to be  $V = V_M$  within the tumour, and  $V = V_N$  elsewhere. We allow for a lag time  $t_0$  between extracellular acid levels changing, and cells mounting the appropriate response of quiescence or proliferation. Under these assumptions, we have

$$\begin{aligned} \frac{\partial H}{\partial t} - D_H \nabla^2 H &:= H_t - D_H (H_R R + 2H_R/R) \\ &= \begin{cases} [(\phi_A - \phi_Q)\theta(H_Q - H(t - t_0)) + \phi_Q] K_M - r_V V_M H & 0 < R < R_M \\ -r_V V_N H & R_M < R, \end{cases} \end{aligned} \tag{1}$$

where  $K_M$  denotes the tumour cell density,  $r_V$  the acid removal rate,  $D_H$  the acid diffusion coefficient and  $\theta$  the Heaviside (or unit step) function defined by

$$\theta(x) = \begin{cases} 0 & x < 0 \\ 1 & x \geq 0. \end{cases} \tag{2}$$

The bracketed term in the second line of Eq. (1) simply represents cells producing acid at rate  $\phi_A$  if  $H(t - t_0) < H_Q$ , and  $\phi_Q$  otherwise.

Taking  $p = \sqrt{r_V V_M / D_H}$ ,  $H_0 = \phi_A K_M / r_V V_M$  and  $T = (r_V V_M)^{-1}$ , and provided the vascular density within the tumour is non-zero (i.e.  $V_M > 0$ ), we may non-dimensionalize Eq. (1) with  $r = pR$ ,  $h = H/H_0$  and  $\tau = t/T$  to obtain

$$h_\tau - (h_{rr} + 2h_r/r) = \begin{cases} (1 - \varepsilon)\theta(h_Q - h(\tau - \tau_0)) + \varepsilon - h & 0 < r < r_M \\ -\psi^2 h & r_M < r, \end{cases} \tag{3}$$

where  $\varepsilon = \phi_Q/\phi_A \ll 1$ ,  $\tau_0 = t_0/T$ ,  $h_Q = H_Q/H_0$ ,  $\psi = \sqrt{V_N/V_M}$  and  $r_M = pR_M$ , subject to continuity of  $h$  and  $h_r$  at  $r = r_M$  and  $\lim_{r \rightarrow \infty} h(r) = 0$ .

Equation (3) can be applied to describe a number of different growth factors besides acidity. Consider, for example, the dynamics of oxygen—from this perspective a positive growth factor consumed by both normal and tumour tissue. Let  $C$  denote the extracellular concentration of oxygen, and suppose that tumour cells cease proliferation when oxygen drops below a threshold concentration  $C_Q$ . Let  $\bar{\phi}_A$ ,  $\bar{\phi}_Q$  and  $\bar{\phi}_N$  be the rates of oxygen consumption by active tumour, quiescent tumour and normal

cells, respectively. We assume that oxygen is supplied through blood vessels at a rate  $\bar{r}_V$ , proportional to the difference between the extracellular oxygen and serum oxygen concentration  $C_S$ . Then we find

$$C_t - D_C (C_R R + 2C_R/R) = \begin{cases} -((\bar{\phi}_A - \bar{\phi}_Q)\theta(C(t-t_0) - C_Q) + \bar{\phi}_Q)K_M + \bar{r}_V V_M (C_S - C) & 0 < R < R_M \\ -\bar{\phi}_N K_N + \bar{r}_V V_N (C_S - C) & R_M < R, \end{cases} \tag{4}$$

where  $D_C$  is the oxygen diffusion coefficient, and  $K_N$  the normal tissue density. Now using the transformations  $h = (C_X - C)/C_0$ ,  $r = \bar{p}R$  and  $\tau = t/\bar{T}$  where

$$\begin{aligned} C_X &= C_S - \frac{\bar{\phi}_N K_N}{\bar{r}_V V_N}, & C_0 &= \frac{(\bar{\phi}_A - \phi_0)K_M}{\bar{r}_V V_M}, & \bar{p} &= \sqrt{\frac{\bar{r}_V V_M}{D_C}}, \\ \bar{T} &= \frac{1}{\bar{r}_V V_M}, & \varepsilon &= \frac{\bar{\phi}_Q - \phi_0}{\bar{\phi}_A - \phi_0}, & \phi_0 &= \frac{\bar{\phi}_N K_N}{\psi^2 K_M}, & \tau_0 &= \frac{t_0}{\bar{T}}, \\ h_Q &= \frac{C_X - C_Q}{C_0}, & \psi &= \sqrt{\frac{V_N}{V_M}}, & r_M &= \bar{p}R_M, \end{aligned} \tag{5}$$

we may recover Eq. (3). Note that this model only makes sense if  $\bar{\phi}_A > \phi_0$ , or equivalently  $\bar{\phi}_A K_M/V_M > \bar{\phi}_N K_N/V_N$ . If this effective rate of active tumour cell oxygen consumption is smaller than the corresponding normal rate, the tumour will receive sufficient oxygen supply, and no regions of hypoxia will occur. One minor difference between the two models is that for acid-induced quiescence we require  $\varepsilon \geq 0$ , whilst for hypoxia-induced quiescence no such restriction is in place.

Through the remainder of this paper, we shall investigate the delay partial differential equation (3). This analysis will allow us to understand the effects of cellular quiescence on cyclical acidosis within tumour tissue.

### 3 Spatial homogeneity

We first consider the dynamics of Eq. (3) in the absence of diffusion. Assuming spatial homogeneity, within the tumour ( $r < r_M$ ) we have

$$\dot{h} = (1 - \varepsilon)\theta(h_Q - h(\tau - \tau_0)) + \varepsilon - h, \tag{6}$$

where the dot denotes the derivative with respect to  $\tau$ . If there is no lag time, i.e.  $\tau_0 = 0$ , then this equation reduces to

$$\dot{h} = (1 - \varepsilon)\theta(h_Q - h) + \varepsilon - h. \tag{7}$$

Looking for steady state solutions to Eq. (7), we see differing behaviours dependent on the value of  $h_Q$ . If  $h_Q > 1$ , then the unique steady state is given by  $h = 1$ , whilst if  $h_Q < \varepsilon$  this steady state is given by  $h = \varepsilon$ . However, if  $h_Q \in (\varepsilon, 1)$ , Eq. (7) has no steady state solution.  $h_\tau > 0$  for  $h < h_Q$  and  $h_\tau < 0$  for  $h > h_Q$ , and thus  $h$  globally converges to  $h_Q$ , even though it is not strictly a steady state solution.

We move on to consider Eq. (6) with a non-zero lag time  $\tau_0$ . Given experimentally determined parameter values of  $p = 4.7 \text{ cm}^{-1}$ ,  $H_0 = 10^{-2} \text{ mM}$  and  $D_H = 1.08 \times 10^{-5} \text{ cm}^2 \text{ s}^{-1}$  [7, 15, 20], we may calculate  $T = 4.2 \times 10^3 \text{ s}$ , meaning that each time unit is equivalent to approximately 1 h. We take  $\varepsilon = 0.01 \ll 1$ , as quiescent cells are essentially metabolically inactive, and  $h_Q = 0.04 \equiv \text{pH } 6.4$  [20]. A change in cellular metabolism in response to a change in extracellular acidity is likely to be mediated by gene transcription and expression. Thus the lag time is likely to be on a similar timescale to that of gene transcription; as such we take  $\tau_0 = 0.5$ , equivalent to a lag of  $t_0 \approx 30 \text{ min}$ . Notice that with this parameter set we find  $h_Q \in (\varepsilon, 1)$ , and thus from the analysis above there is no steady state and we would expect non-equilibrium dynamics.

For  $h_Q \in (\varepsilon, 1)$ , Eq. (6) has analytical solution

$$h = \begin{cases} 1 - (1 - h_Q)e^{-\tau} & h \text{ increasing} \\ \varepsilon + (h_Q - \varepsilon)e^{-\tau} & h \text{ decreasing,} \end{cases} \tag{8}$$

where  $\tau$  is shifted such that  $\tau = 0$  corresponds to  $h = h_Q$ . The maximum and minimum acid levels are given, respectively, by substituting  $\tau = \tau_0$  above.

In Fig. 1 we present results for the spatially homogeneous model of tumour acidity, using the typical parameter values above. Cycles of acidosis are observed; the acid levels vary between their maximum level of  $h \approx 0.42 \equiv \text{pH } 5.4$  to their minimum level of  $h \approx 0.028 \equiv \text{pH } 6.5$ .

The time from minimum acidity to  $h_Q$  ( $A \rightarrow B$  in Fig. 1) is given by

$$\tau_1 = \log \left( \frac{1 - \varepsilon - (h_Q - \varepsilon)e^{-\tau_0}}{1 - h_Q} \right) \approx 0.01, \tag{9}$$

whilst the time from maximum acidity to  $h_Q$  ( $C \rightarrow D$ ) is given by

$$\tau_2 = \log \left( \frac{1 - \varepsilon - (1 - h_Q)e^{-\tau_0}}{h_Q - \varepsilon} \right) \approx 2.6. \tag{10}$$

The total cycle time is

$$\tau_c = 2\tau_0 + \tau_1 + \tau_2 = \log \left[ \left( e^{\tau_0} \frac{1 - \varepsilon}{h_Q - \varepsilon} - 1 \right) \left( e^{\tau_0} \frac{1 - \varepsilon}{1 - h_Q} - 1 \right) \right] \approx 3.6, \tag{11}$$

equivalent to approximately 4 h.

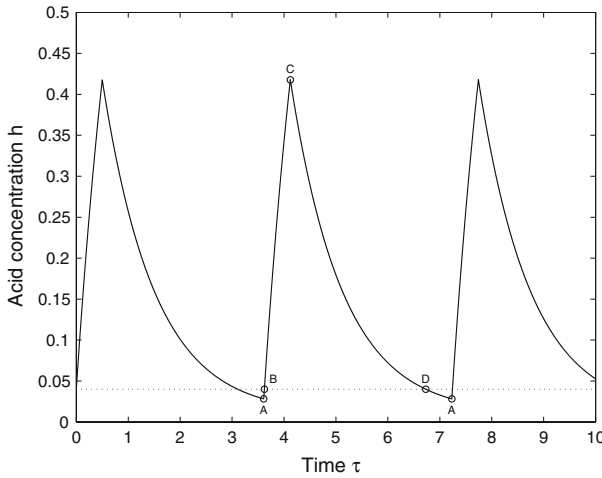


**Fig. 1** Results from Eq. (8). Predicted cyclical acidosis for the spatially homogeneous model, using typical parameter values  $h_Q = 0.04$ ,  $\varepsilon = 0.01$  and  $\tau_0 = 0.5$  and initial conditions  $h(t) = h_Q$  for  $\tau \in [-\tau_0, 0]$ . The acid level cycles around  $h_Q$  (dotted line), between its maximum value of  $h \approx 0.42$  and minimum value of  $h \approx 0.028$ . The time for each of the steps  $A \rightarrow B \rightarrow C \rightarrow D \rightarrow A$  is given by  $\tau_1 \approx 0.01$ ,  $\tau_0$ ,  $\tau_2 \approx 2.6$  and  $\tau_0$ , respectively. The total cycle time is approximately 3.6 non-dimensional units

### 4 Temporal homogeneity

Typically, the first step we take when investigating the role of a specific metabolite in tumour development is to look for temporally-homogeneous solutions to the metabolite evolution equation. The justification for this is that the timescale of metabolite diffusion ( $\sim$  minutes) is much less than the timescale of, for example, tumour growth ( $\sim$  days), and hence the metabolite can be assumed to be in diffusive equilibrium. This removes the need for both the metabolite evolution term  $\partial h / \partial \tau$  and the lag term  $\tau_0$ .

Assuming temporal homogeneity, Eq. (3) reduces to

$$r^2 h'' + 2r h' = \begin{cases} r^2 h - ((1 - \varepsilon)\theta(h_Q - h) + \varepsilon)r^2 & 0 < r < r_M \\ \psi^2 r^2 h & r_M < r, \end{cases} \quad (12)$$

where the primes denote the derivative with respect to  $r$ .

We may solve Eq. (12) for  $r_M < r$ ; applying continuity of  $h$  and its derivative at  $r_M$  we find that within the tumour

$$r^2 h'' + 2r h' = r^2 h - ((1 - \varepsilon)\theta(h_Q - h) + \varepsilon)r^2 \quad 0 < r < r_M, \quad (13)$$

subject to the boundary conditions

$$h'(0) = 0, \quad h'(r_M) = -h(r_M) \frac{1 + \psi r_M}{r_M}. \quad (14)$$

The second boundary condition arises from the solution  $h = Ae^{-\psi r}/r$ , for some constant  $A$ , in the outer region  $r_M < r$ .

We will now move on to show that, if  $h_Q \in (\varepsilon, 1)$  and  $r_M$  is sufficiently large, Eq. (13) has no solution. Consider first a tumour in which all cells are active. Then, from Eqs. (13) and (14)

$$r^2h'' + 2rh' - r^2h + r^2 = 0, \tag{15}$$

which, subject to the boundary conditions in Eq. (14) has solution

$$h(r) = 1 - k_1 \frac{\sinh r}{r}, \tag{16}$$

where

$$k_1 = \frac{1 + \psi r_M}{\cosh r_M + \psi \sinh r_M}. \tag{17}$$

In particular

$$h(0) = 1 - k_1 \rightarrow 0 \text{ as } r_M \rightarrow 0, \quad h(0) \rightarrow 1 \text{ as } r_M \rightarrow \infty. \tag{18}$$

Thus, if  $h_Q < 1$ , at some radius  $r_M = r^*$ ,  $h(0) = h_Q$  and the cells at the tumour centre will become quiescent. This radius  $r^*$  may be found numerically from the expression above for  $h(0)$ , i.e. through solution of

$$\psi r^* = (1 - h_Q)(\cosh r^* + \psi \sinh r^*) - 1. \tag{19}$$

For typical parameter values  $h_Q = 0.04$  and  $\psi = 1$ , we find  $r^* = 0.31$ , equivalent to the first quiescent cells appearing when the tumour has radius  $R \approx 0.7$  mm.

Assuming that  $r_M > r^*$ , some of the tumour cells must be quiescent. Suppose  $h_Q \in (\varepsilon, 1)$  and consider a region  $(r_1, r_2)$  containing only quiescent cells, i.e. a region where  $h > h_Q$  everywhere. Then, from Eq. (13) within this region

$$r^2h'' + 2rh' - r^2h + \varepsilon r^2 = 0. \tag{20}$$

The edges of the region  $r_1$  and  $r_2$  must either be a tumour boundary (0 or  $r_M$ ) and satisfy the appropriate condition in Eq. (14) or they must satisfy  $h(r_i) = h_Q$ . We consider each case separately below.

*Case I:*  $r_1 = 0, r_2 = r_M$ .

Consider the case where all the cells in the tumour are quiescent. Then, applying the boundary conditions in Eq. (14),

$$h(r) = \varepsilon \left( 1 - k_1 \frac{\sinh r}{r} \right), \tag{21}$$

where, in particular

$$h(0) = \varepsilon(1 - k_1) < \max(\varepsilon, 0) < h_Q. \tag{22}$$

This contradicts the fact that the whole tumour is quiescent.

Case 2:  $r_1 = 0, h(r_2) = h_Q$ .

Consider now the case where the quiescent cells are limited to the tumour centre. Then in  $(0, r_2)$

$$h(r) = \varepsilon + \left[ (h_Q - \varepsilon) \frac{r_2}{\sinh r_2} \right] \frac{\sinh r}{r}, \tag{23}$$

where, in particular

$$h(0) = \varepsilon + (h_Q - \varepsilon) \frac{r_2}{\sinh r_2} < h_Q, \tag{24}$$

as  $r_2/\sinh r_2 \in (0, 1)$ , again contradicting the fact that cells at the tumour centre are quiescent.

Case 3:  $h(r_1) = h_Q$ .

Suppose finally that the cells in the tumour centre  $(0, r_1)$  are active ( $h < h_Q$ ) and surrounded by quiescent cells. Then  $h(r_1) = h_Q$  and, in  $(0, r_1)$ ,

$$h(r) = 1 - \left[ (1 - h_Q) \frac{r_1}{\sinh r_1} \right] \frac{\sinh r}{r}, \tag{25}$$

where, in particular

$$h(0) = 1 - (1 - h_Q) \frac{r_1}{\sinh r_1} > h_Q, \tag{26}$$

contradicting the fact that the cells at the tumour centre are active.

The analysis presented above has shown that, when  $r_M > r^*$  and  $h \in (\varepsilon, 1)$ , Eq. (12) has no solution. As such, the standard assumption of temporal homogeneity is not valid; instead we must consider the temporal dynamics of the system. In the previous section we showed that when  $h \in (\varepsilon, 1)$ , the assumption of spatial homogeneity leads to cyclical solutions. Given this evidence, for the full model defined in Eq. (3), we expect cyclical behaviour to occur whenever  $r_M > r^*$  and  $h \in (\varepsilon, 1)$ . This behaviour is analysed in the next section.

### 5 Full model analysis

We move on to analyse the full model, including both temporal and spatial dynamics. The model is defined by Eq. (3), which we reiterate here

$$h_\tau - (h_{rr} + 2h_r/r) = \begin{cases} (1 - \varepsilon)\theta(h_Q - h(\tau - \tau_0)) + \varepsilon - h & 0 < r < r_M \\ -\psi^2 h & r_M < r, \end{cases} \tag{27}$$

subject to the boundary conditions  $h_r(0, \tau) = 0$ , continuity of  $h$  and  $h_r$  at  $r = r_M$  and  $\lim_{r \rightarrow \infty} h(r, \tau) = 0$ , and initial conditions  $h(r, \tau) = 0$  for  $\tau \in [-\tau_0, 0]$ .

The method of lines [17] is a technique that may be applied to numerically solve parabolic equations, involving discretizing in all but one dimension, and then integrating the semi-discrete problem as a system of ordinary differential equations (ODEs).

The method allows us to take advantage of the sophisticated tools available for numerical solution of ODEs and, in this case, delay (ordinary) differential equations (DDEs).

We discretize Eq. (27) with respect to the variable  $r$  using finite differences, in particular using the approximations

$$\begin{aligned}
 h_r(r, \tau) &\approx \frac{h(r + \Delta, \tau) - h(r - \Delta, \tau)}{2\Delta} \\
 h_{rr}(r, \tau) &\approx \frac{h(r + \Delta, \tau) + h(r - \Delta, \tau) - 2h(r, \tau)}{\Delta^2},
 \end{aligned}
 \tag{28}$$

for small  $\Delta$ .

To use the discretization above, we first approximate the infinite domain  $[0, \infty)$  as a finite domain  $[0, r_\infty]$ , where  $r_\infty = kr_M$  for some integer  $k > 1$ . The boundary condition at  $r = \infty$  is then replaced by the condition  $h(r_\infty, \tau) = 0$ . We then choose a uniform grid  $r_j, j = 1, \dots, kN$  with spacing  $\Delta = r_\infty/kN = r_M/N$  such that  $r_j = j\Delta$ . This allows us to define  $h_j(\tau) = h(r_j, \tau)$  to be the value of  $h$  at each of these grid points.

The Dirichlet boundary condition  $h(r_\infty, \tau) = 0$  is handled easily by defining  $h_{kN}(\tau) = 0$ . The Neumann boundary condition  $h_r(0, \tau) = 0$  requires more care. We first apply l'Hôpital's rule to obtain

$$\lim_{r \rightarrow 0} \frac{h_r(r, \tau)}{r} = \lim_{r \rightarrow 0} \frac{[h_r(r, \tau)]_r}{[r]_r} = h_{rr}(0, \tau).
 \tag{29}$$

To handle this second order difference, imagine the problem is instead being solved on the domain  $[-r_\infty, r_\infty]$ , with the tumour tissue confined to  $[-r_M, r_M]$  and the same boundary conditions at  $r = \pm r_\infty$ . The Neumann boundary condition then implies that the solution will be symmetric with respect to  $r$  for all time. Thus  $h(-\Delta, \tau) = h(\Delta, \tau)$ , so  $h_{-1}(\tau) = h_1(\tau)$ .

The system of  $(kN + 1)$  DDEs in the variable  $\tau$  is then given by

$$h'_j = \begin{cases} 6[h_1 - h_0]\Delta^{-2} + f_0 & j = 0 \\ [(1 + j^{-1})h_{j+1} + (1 - j^{-1})h_{j-1} - 2h_j]\Delta^{-2} + f_j & j = 1, \dots, N \\ [(1 + j^{-1})h_{j+1} + (1 - j^{-1})h_{j-1} - 2h_j]\Delta^{-2} - \psi^2 h_j & j = N+1, \dots, kN-1 \\ 0 & j = kN, \end{cases}
 \tag{30}$$

where

$$f_j(\tau) = (1 - \varepsilon)\theta(h_Q - h_j(\tau - \tau_0)) + \varepsilon - h_j(\tau).
 \tag{31}$$

The system of DDEs in Eq. (30) is solved using the MATLAB® integrator `dde23` [22]. Preliminary tests showed that  $k = 5$  was a suitable choice—integrating over domains larger than  $[0, 5r_M]$  had a negligible effect on the system solution.

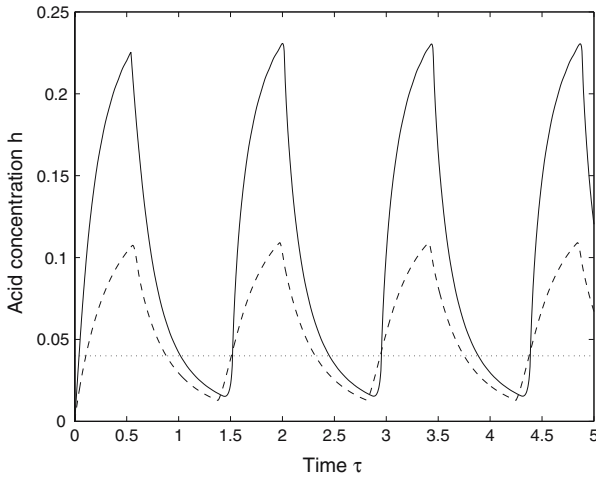


**Fig. 2** Results from Eq. (30). Cycles of acidity observed at the tumour centre (*solid line*) and tumour edge (*dashed line*) for the full model, using typical parameter values  $h_Q = 0.04$ ,  $\varepsilon = 0.01$ ,  $\psi = 1$ ,  $\tau_0 = 0.5$  and  $r_M = 1$ . The domain of integration used is  $[0, 5r_M]$ , divided into 251 grid points. The acidity levels cycle around the quiescence threshold  $h_Q$  (*dotted line*), with cycle time of approximately 1.4 units

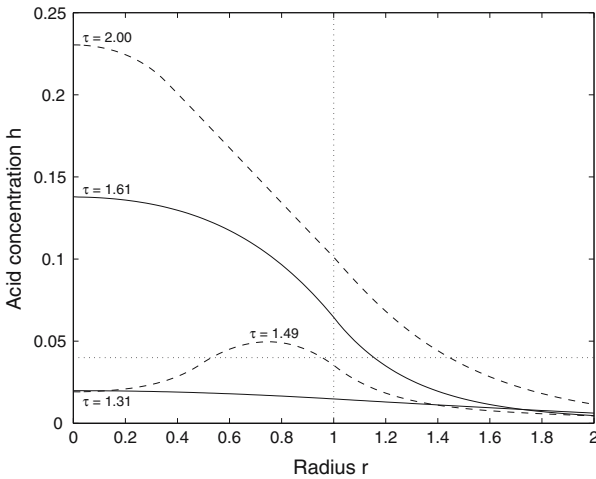


**Fig. 3** Changing acid profiles in and around the tumour during the acidosis cycle as depicted in Fig. 2. Notice that for some of this cycle, acidity is higher at the tumour edge than centre. Parameter values used are as in Fig. 2. The *dotted lines* represent the tumour radius ( $r_M = 1$ ) and quiescence threshold ( $h_Q = 0.04$ )

Typical model solutions are shown in Figs. 2 and 3. Given typical parameter values of  $h_Q = 0.04$  and  $\psi = 1$ , we may calculate from Eq. (19)  $r^* = 0.31$ , the tumour radius at which quiescence first occurs. Choosing  $r_M = 1 > r^*$  and  $\varepsilon = 0.01$ , we have  $h_Q \in (\varepsilon, 1)$ , and thus, from previous analyses, we would expect cyclical acidosis to occur.

Figure 2 shows cyclical acidity at the tumour centre and tumour edge using these parameter values. The cells at the tumour centre cycle between their maximum level of  $h \approx 0.23 \equiv \text{pH } 5.6$  and their minimum level  $h \approx 0.016 \equiv \text{pH } 6.7$ . The cells at the tumour edge also experience cyclical acidity about the quiescence threshold, though their maximum acidity  $h \approx 0.11 \equiv \text{pH } 5.9$  is less than the cells at the centre. The cycle time is  $\tau_c \approx 1.4$ , equivalent to 100 min.

This may be compared to the spatially homogeneous model presented in Fig. 1. Addition of diffusion to the model acts to smooth the spatial profile of the dynamics, reducing the maximum acidity levels seen and in turn decreasing the acid cycle time. Intuitive understanding of the reasons for the reduction in cycle time may be gained through approximation of peritumoural acid diffusion and removal as a simple damping effect on the spatially homogeneous system. Including this in Eq. (6), we have

$$\dot{h} = (1 - \varepsilon)\theta(h_Q - h(\tau - \tau_0)) + \varepsilon - h - \kappa h, \tag{32}$$

where the term  $-\kappa h$  represents the additional role of diffusion. Through a suitable transformation, we may recover Eq. (6), and hence an analogous definition for cycle time, valid if  $h_Q(1 + \kappa) \in (\varepsilon, 1)$

$$\tau_c = \frac{1}{1 + \kappa} \log \left[ \left( e^{\tau_0(1+\kappa)} \frac{1 - \varepsilon}{h_Q(1 + \kappa) - \varepsilon} - 1 \right) \left( e^{\tau_0(1+\kappa)} \frac{1 - \varepsilon}{1 - h_Q(1 + \kappa)} - 1 \right) \right]. \tag{33}$$

At our default parameter values,  $\partial\tau_c/\partial\kappa < 0$  at  $\kappa = 0$ , and thus damping acts to reduce cycle time. By equating Eq. (33) with our known cycle time of  $\tau_c = 1.4$  in the presence of diffusion, we find an effective damping coefficient of  $\kappa \approx 3.6$ .

In Fig. 3 we investigate how acidity levels vary through the tumour during each cycle. Initially, all the cells within the tumour are below the quiescence threshold. Cycles of acidity are out of phase for different sections of the tumour and an increase in acidity is first seen at the tumour edge ( $r = 1$ ). Acidity then increases at the tumour centre ( $r = 0$ ), before reaching its maximum level. This figure demonstrates that, whilst acid levels are on average higher in the tumour centre than the tumour edge, this property does not hold for all points in the acid cycle. The point is reinforced in Fig. 4, which shows how the metabolic characteristics of tumour cells vary during each cycle. The first cells to become quiescent due to high extracellular acidity are not at the tumour centre, rather this occurs at  $r \approx 0.81$  near the edge of the tumour.

## 6 Discussion

Fluctuations in metabolite levels are known to occur within tumours with discrete periodicities of hours, minutes and days. Cells that are best suited to respond to these periods of cellular stress, such as through constitutive upregulation of aerobic glycolysis, will be positively selected by somatic evolutionary forces. These cycles are assumed to occur due to haemodynamic variations such as changes in the local concentration of red blood cells or structural rearrangement of blood vessels. In this paper

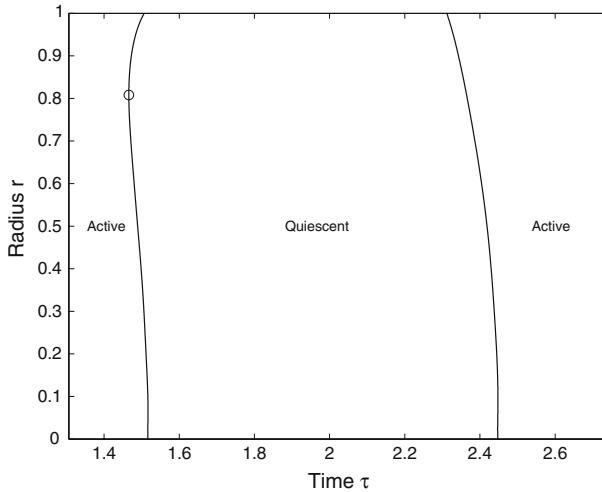


**Fig. 4** Changing metabolic characteristics during the acidosis cycle as depicted in Figs. 2 and 3. The first cells to become quiescent are located at  $r \approx 0.81$ , whilst the first cells to resume proliferation are at the tumour edge,  $r = 1$ . For the majority of the cycle, the whole of the tumour is in the same metabolic state, with all cells either active or quiescent. Parameter values used are as in Fig. 2

we have investigated a further hypothesis, namely that quiescence in response to cellular stress, and the corresponding drop in metabolism, provides a negative feedback mechanism capable of reproducing such metabolite cycles.

A simple reaction–diffusion system is used to describe the evolution of the metabolite of interest. Whilst we focus on the dynamics of acidity within the tumour, the model is equally valid for any growth inhibitor produced by tumour cells or any growth promoter consumed by tumour cells.

Many existing models of both in vitro and in vivo tumour growth [3,6,16,21], essentially extensions of the original model of Greenspan [11], describe the evolution of the tumour outer boundary in response to vital nutrients and growth factors. These models vary greatly in their complexity and application, including viscosity, migration or cell cycle considerations, for example. Despite this diversity, each model has in common the assumption that, over the timescale of interest such as cellular proliferation, the metabolites in the system will be in diffusive equilibrium. Here we have shown, for a biologically realistic range of parameter values ( $r_M > r^*$  and  $h_Q \in (\varepsilon, 1)$ ), that this standard assumption is not valid. Rather, when investigating the distribution of metabolites around a vascularised tumour in which cellular quiescence occurs, temporal dynamics must be considered.

We first investigate a spatially homogeneous model, and find that cycles of acidity due to cellular quiescence occur with a periodicity of around 4 h. Inclusion of spatial aspects and diffusion reduces this cycle time to between 1 and 2 h, consistent with experimental evidence [12]. Within the parameter regime used here we find the acid levels at the tumour centre will oscillate between pH 5.6 and 6.7.

Given the importance of acidic and hypoxic cycles in mediating the evolution of cancer cell metabolism and resistance to acidity, further experimental verification of the role of quiescence in inducing metabolic cycles will be of considerable interest.

## References

- Baudelet, C., Ansiaux, R., Jordan, B., Havaux, X., Macq, B., Gallez, B.: Physiological noise in murine solid tumours using T2\*-weighted gradient-echo imaging: a marker of tumour acute hypoxia? *Phys. Med. Biol.* **49**, 3389–3411 (2004)
- Braun, R., Lanzen, J., Dewhirst, M.: Fourier analysis of fluctuations of oxygen tension and blood flow in R3230Ac tumors and muscle in rats. *Am. J. Physiol.* **277**, H551–H568 (1999)
- Byrne, H.: A weakly nonlinear analysis of a model of avascular solid tumour growth. *J. Math. Biol.* **39**, 59–89 (1999)
- Casciari, J., Sotirchos, S., Sutherland, R.: Variations in tumor cell growth rates and metabolism with oxygen concentration, glucose concentration, and extracellular pH. *J. Cell. Physiol.* **151**, 386–94 (1992)
- Dewhirst, M., Kimura, H., Rehmus, S., Braun, R., Papahadjopoulos, D., Hong, K., Secomb, T.: Microvascular studies on the origins of perfusion-limited hypoxia. *Br. J. Cancer Suppl.* **27**, S247–S251 (1996)
- Franks, S., Byrne, H., Underwood, J., Lewis, C.: Biological inferences from a mathematical model of comedo ductal carcinoma in situ of the breast. *J. Theor. Biol.* **232**, 523–543 (2005)
- Gatenby, R., Gawlinski, E.: A reaction–diffusion model of cancer invasion. *Cancer Res.* **56**, 5745–5753 (1996)
- Gatenby, R., Gillies, R.: Why do cancers have high aerobic glycolysis? *Nat. Rev. Cancer* **4**, 891–899 (2004)
- Gilead, A., Neeman, M.: Dynamic remodeling of the vascular bed precedes tumor growth: MLS ovarian carcinoma spheroids implanted in nude mice. *Neoplasia* **1**, 226–230 (1999)
- Goda, N., Ryan, H., Khadivi, B., McNulty, W., Rickert, R., Johnson, R.: Hypoxia-inducible factor 1 $\alpha$  is essential for cell cycle arrest during hypoxia. *Mol. Cell. Biol.* **23**, 359–369 (2003)
- Greenspan, H.: Models for the growth of a solid tumor by diffusion. *Stud. Appl. Math.* **51**, 317–340 (1972)
- Hill, R., De Jaeger, K., Jang, A., Cairns, R.: pH, hypoxia and metastasis. *Novartis Found. Symp.* **240**, 154–165 (2001)
- Kiani, M., Pries, A., Hsu, L., Sarelius, I., Cokelet, G.: Fluctuations in microvascular blood flow parameters caused by hemodynamic mechanisms. *Am. J. Physiol.* **266**, H1822–H1828 (1994)
- Kimura, H., Braun, R., Ong, E., Hsu, R., Secomb, T., Papahadjopoulos, D., Hong, K., Dewhirst, M.: Fluctuations in red cell flux in tumor microvessels can lead to transient hypoxia and reoxygenation in tumor parenchyma. *Cancer Res.* **56**, 5522–5528 (1996)
- Martin, G., Jain, R.: Noninvasive measurement of interstitial pH profiles in normal and neoplastic tissue using fluorescence ratio imaging microscopy. *Cancer Res.* **54**, 5670–4 (1994)
- McElwain, D., Morris, L.: Apoptosis as a volume loss mechanism in mathematical models of solid tumor growth. *Math. Biosci.* **39**, 147–157 (1978)
- Mikhlin, S., Smolitsky, K.: *Approximate Methods for the Solution of Differential and Integral Equations*. Elsevier, Amsterdam (1967)
- Murphy, M., Carlson, J., Keough, M., Claffey, K., Signoretti, S., Loda, M.: Hypoxia regulation of the cell cycle in malignant melanoma: putative role for the cyclin-dependent kinase p27<sup>kip1</sup>. *J. Cutan. Pathol.* **31**, 477–482 (2004)
- Patan, S., Tanda, S., Roberge, S., Jones, R., Jain, R., Munn, L.: Vascular morphogenesis and remodeling in a human tumor xenograft: blood vessel formation and growth after ovariectomy and tumor implantation. *Circ. Res.* **89**, 732–739 (2001)
- Patel, A., Gawlinski, E., Lemieux, S., Gatenby, R.: A cellular automaton model of early tumor growth and invasion. *J. Theor. Biol.* **213**, 315–31 (2001)
- Pettet, G., Please, C., Tindall, M., McElwain, D.: The migration of cells in multicell tumor spheroids. *Bull. Math. Biol.* **63**, 231–257 (2001)
- Shampine, L., Thompson, S.: Solving DDEs in MATLAB. *Appl. Numer. Math.* **37**, 441–458 (2001)
- Smallbone, K., Gatenby, R., Gillies, R., Maini, P., Gavaghan, D.: Metabolic changes during carcinogenesis: potential impact on invasiveness. *J. Theor. Biol.* **244**, 703–713 (2007)
- Smallbone, K., Gavaghan, D., Gatenby, R., Maini, P.: The role of acidity in solid tumor growth and invasion. *J. Theor. Biol.* **235**, 476–484 (2005)
- Sonveaux, P., Dessy, C., Martinive, P., Havaux, X., Jordan, B., Gallez, B., Gregoire, V., Balligand, J., Feron, O.: Endothelin-1 is a critical mediator of myogenic tone in tumor arterioles: implications for cancer treatment. *Cancer Res.* **64**, 3209–3214 (2004)
- Warburg, O.: *The Metabolism of Tumours*. Constable Press, London (1930)